Evidence for speed sensitivity to motion in depth from binocular cues

Susan G. Wardle

School of Psychology, The University of Sydney, Sydney, NSW, Australia

David Alais

School of Psychology, The University of Sydney, Sydney, NSW, Australia

Motion in depth can be perceived from binocular cues alone, yet it is unclear whether these cues support speed sensitivity in the absence of the monocular cues that normally co-occur in natural viewing. We measure threshold contours in space-time for the discrimination of three-dimensional (3D) motion to determine whether observers use speed to discriminate a test 3D motion from two identical standards. We compare thresholds for random-dot stereograms (RDS) containing both binocular cues to 3D motion—interocular velocity difference and changing disparity over time—with performance for dynamic random-dot stereograms (DRDS), which contain only the second cue. Threshold contours are tilted along the axis of constant velocity in space-time for RDS stimuli at slow speeds (0.5 m/s), evidence for speed sensitivity. However, for higher speeds (1.5 m/s) and DRDS stimuli, observers rely on the component cues of duration and disparity. In a second experiment, noise of constant velocity is added to the standards to degrade the reliability of these separate components. Again there is evidence for speed tuning for RDS, but not for DRDS. Considerable variation is observed in the ability of individual observers to use the different cues in both experiments, however, in general the results emphasize the importance of interocular velocity difference as a critical cue for speed sensitivity to motion in depth, and suggest that speed sensitivity to stereomotion from binocular cues is restricted to relatively slow speeds.

Keywords: stereomotion, speed discrimination, binocular vision, interocular velocity difference, 3D motion

Citation: Wardle, S. G., & Alais, D. (2013). Evidence for speed sensitivity to motion in depth from binocular cues. *Journal of Vision, 13*(1):17, 1–16, http://www.journalofvision.org/content/13/1/17, doi:10.1167/13.1.17.

Introduction

Under natural viewing conditions, motion in depth produces a combination of monocular and binocular cues that can be used by the visual system to detect the trajectory and speed of objects moving towards or away from the observer. However, it is possible to perceive movement in depth from binocular cues alone. An object moving along the *z*-axis creates two binocular cues that are potentially useful for detecting motion in depth (Cumming & Parker, 1994; Rashbass & Westheimer, 1961; Regan, 1993). The first is a change in the binocular disparity of the object that is either receding (increasing the binocular disparity between each eye's view, relative to fixation) or approaching (which reduces disparity). The other cue is the interocular velocity difference of the horizontal motion of the object across the two retinae. There is substantial evidence that changing disparity over time and interocular velocity differences are both used by the visual system to perceive motion in depth (see Harris, Nefs, & Grafton, 2008 for a review) and recent fMRI evidence indicates that both cues are processed in human MT+ (Rokers, Cormack, & Huk, 2009). Results from different tasks suggest that the two cues are not weighted equally, and their relative importance remains controversial (Beverley & Regan, 1973; Brooks, 2002; Brooks & Stone, 2004, 2006, 2010; Cumming & Parker, 1994; Czuba, Rokers, Huk, & Cormack, 2010; Czuba, Rokers, Guillet, Huk, & Cormack, 2011; Fernandez & Farell, 2005; Nefs & Harris, 2010; Nefs, O'Hare & Harris, 2010; Regan & Gray, 2009; Sakano, Allison, & Howard, 2012; Shioiri, Saisho, & Yaguchi, 2000; Sumnall & Harris, 2000).

The aim of this paper is to determine whether there are speed mechanisms for three-dimensional (3D) motion that are tuned to speed per se. The existing literature is contradictory. Harris and Watamaniuk (1995) found that speed discrimination for motion in depth was as good as that for monocular motion when monocular cues and both binocular cues were available. The stimulus was a random-dot stereogram with the central square receding in depth. However, speed discrimination was much worse when monocular motion cues were removed by using a dynamic random-dot stereogram, in which the random dots changed each frame, leaving only disparity-defined motion signals. The Weber fractions across observers

doi: 10.1167/13.1.17 Received June 16, 2012; published January 10, 2013 ISSN 1534-7362

were in the range 0.1–0.2 for monocular motion or motion-in-depth with monocular cues, and elevated to 0.40–0.56 for the cyclopean stimulus. Their analysis also suggested that observers were using a position cue based on static disparity in the cyclopean stimulus for the speed discrimination task. This would indicate that changing disparity was a poor cue for speed discrimination in the task, and led the authors to conclude that there is no specific stereo-speed mechanism. They later replicated this result for translational motion of a cyclopean grating in the *xy* plane, as speed discrimination was also poor when changing disparity was the only cue (Harris & Watamaniuk, 1996).

This result has been contradicted by other studies. Portfors-Yeomans and Regan (1996) found speed discrimination towards or away from the observer did not differ for cyclopean and noncyclopean motion-in-depth stimuli. The lowest Weber fractions were 0.12 and 0.1 respectively, and their regression analysis indicated that observers were appropriately using the speed cue for the speed task, rather than a positional disparity cue. The authors suggest that the reason for the difference between their results and that of Harris and Watamaniuk (1995) is because the earlier study used a cyclopean target, which disappeared partway through the motion path as it passed through a reference frame of dots at zero disparity. Portfors-Yeomans and Regan (1996) used a disparity pedestal so the cyclopean stimuli were visible for the entire motion trajectory. This suggestion is supported by a control experiment in which Portfors-Yeomans and Regan (1996) allowed the cyclopean-defined motion to pass through zero disparity. In this case they also reported elevated cyclopean speed discrimination Weber fractions (0.16–0.22 across observers) compared to non-cyclopean stimuli (0.12–0.15). Although this agrees with the data of Harris and Watamaniuk (1995), the degree of elevation for cyclopean motion was considerably less. Brooks and Stone (2004) suggested a possible reason for the lack of a difference between cyclopean and non-cyclopean stimuli in Portfors-Yeomans and Regan (1996) may be an inadequate interocular velocity cue in their stimulus. Portfors and Regan (1997) also reported low discrimination thresholds for cyclopean stimuli, both for motion in depth and cyclopean translational motion in the *xy* plane. They concluded that there are two separate stereo motion mechanisms: one sensitive to speed and the other to the excursion in depth.

A difficulty in determining whether there are speed mechanisms for stereomotion is the problem of experimentally separating the component cues. Speed in the stereo domain is described as a change in disparity over time: $s = \Delta d/\Delta t$. Because of this relationship, if one component is held constant, the other two vary, and consequently their effects on experimental observations such as thresholds are conflated. Typically studies of speed discrimination for motion in depth attempt to control for these components indirectly, for example by randomizing stimulus duration (Brooks & Stone, 2004; Harris & Watamaniuk, 1995), changing the 3D motion trajectory to decouple monocular image speed and motion in depth speed (Brooks & Stone, 2004; Harris & Watamaniuk, 1995) or by comparing performance against control conditions in which only static disparity (e.g., the first and last frames of a motion stimulus) is shown (Harris & Watamaniuk, 1995). To address this issue, we adapt an elegant paradigm from Reisbeck and Gegenfurtner (1999) that they applied to luminance-defined motion. As explained below, the power of this paradigm is that it allows for the separation of space, time, and speed.

The paradigm used by Reisbeck and Gegenfurtner (1999) maps motion discrimination thresholds as a two-dimensional (2D) contour in space-time coordinates. In our adaptation of Reisbeck and Gegenfurtner's (1999) method, space and time correspond to a change in disparity and a change in duration, relative to the parameters of a standard stimulus. Note that because disparity and duration are in different units, measurements in the stimulus space are calculated in terms of Weber fractions. Thus the *x* and *y* axes in the stimulus space (shown in Figure 1) are *dimensionless Weber fractions*, and hence the only line of constant velocity is at 45°. This should not be confused with a linear space-time coordinate system, in which any straight line would represent a line of constant velocity.

The task is a three interval "odd-one-out" discrimination relative to a standard motion stimulus with fixed spatial, temporal and speed parameters. Thresholds for the just-noticeable difference (JND) compared to the standard are measured for 16 different combinations of space and time. This forms a 2D threshold contour (Figure 1a). The shape of the threshold contour reflects the nature of the underlying visual mechanisms. If the mechanisms are space-time separable, the contour will be aligned horizontally or vertically with the space-time axes, depending on which cue is more useful for discrimination (Figure 1b, c). However, if there is speed sensitivity to motion in depth, discrimination performance will be worse when the tested direction is a constant ratio of space-time (i.e., at a constant velocity) relative to the standard. This would produce a threshold contour tilted on the Cartesian plane along the line of constant velocity (Figure 1d). The line of constant velocity relative to the parameters of the standard stimulus is tilted at 45° in space-time and passes through the parameters of the reference stimulus (marked by the red line in Figure 1a).

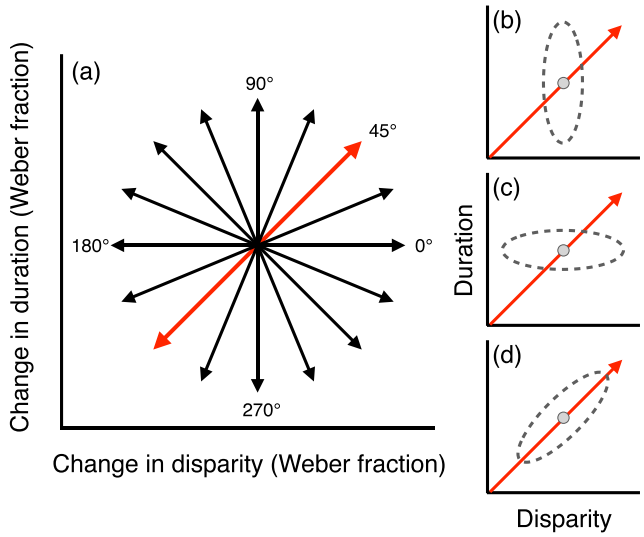

Figure 1. Predictions of underlying visual mechanisms from the shape of 2D motion-in-depth discrimination contours. The center of each plot represents the fixed parameters of the standard stimulus in space-time and the red line at 45° is the line of constant velocity relative to the parameters of the standard. The *x* and *y* axes are *dimensionless Weber fractions,* which represent changes in disparity or duration relative to the parameters of the standard. (a) Thresholds were measured in 16 directions (θ) away from the standard to form a 2D threshold contour. Panels b, c, and d show potential outcomes. (b) A vertical ellipse results if space-time mechanisms are separable and disparity is the more useful cue. (c) A horizontal ellipse results if space-time mechanisms are separable and duration is more useful. (d) Speed-tuned mechanisms would cause the contour to be tilted at 45° along the line of constant velocity.

In the first experiment we derived the threshold contours for two standard speeds of motion in depth to examine whether there are specific binocular mechanisms tuned to speed. To isolate purely cyclopean mechanisms, we used a dynamic random-dot stimulus (DRDS) in which the random dots change over time, so there is 100% interocular correlation of the dots on each frame, but 0% temporal correlation, thus eliminating the interocular velocity cue (Julesz, 1971). We compared these data to conventional random-dot stereograms (RDS), which are not dynamically updated and so include both binocular cues for motion in depth – interocular velocity difference (IOVD) and changing disparity over time. RDS and DRDS stimuli produce equivalent detection (Cumming & Parker, 1994) and stereoacuity (Brooks & Stone, 2004, 2006) thresholds, although the RDS stimulus is not cyclopean because horizontal retinal motion of the central stimulus can be detected between monocular images. In the second experiment we measured discrimination thresholds when spatiotemporal noise was added to the standard stimuli, with the aim to better isolate potential speed mechanisms by degrading the reliability of the component cues of duration and disparity (see Methods for Experiment 2).

Experiment 1

Method

Observers

Three observers participated; all had normal stereo vision and normal or corrected-to-normal visual acuity. One observer was an author (SW); the other two observers (CL, NM) were naive to the aims of the experiment and received financial reimbursement for their participation. The experimental procedure was conducted in accordance with the Declaration of Helsinki.

Apparatus and stimuli

Stereoscopic stimuli were generated on an Apple Mac Pro 4.1 computer using MATLAB (The MathWorks) with functions from the Psychtoolbox (Brainard, 1997; Pelli, 1997). Stimuli were presented on two identical Viewsonic Professional Series P225f CRT monitors at 120 Hz with screen resolution 1056 × 792 pixels. The monitors were gamma-corrected to obtain linear output from each RGB gun. Subpixel resolution via anti-aliasing on the graphics card provided a spatial positioning accuracy of 0.016 of a pixel, corresponding to a stereoscopic resolution of 0.55 arcsec. Observers viewed the stimuli through a mirror stereoscope, with each monitor displaying one eye's image.

The motion-in-depth stimuli were random dot patterns (4.9° × 4.9°) presented on a gray screen of mean luminance. An example stereogram of the stimulus is in Figure 2. The stimulus consisted of two superimposed dot patterns (the central foreground and the background), each contained 50% black and 50% white dots with a dot density of 21 dots per deg^2. Individual dots were circles 4 arcmin in diameter (there is evidence that motion in depth simulation is more accurate with constant dot sizes between 2.2–4.4 arcmin; see Gray & Regan, 1999). The background dots served as a reference frame for the 3D motion stimulus. The rectangular area of 3D motion dots [2.4° (H) × 6.8° (W)] was centered on the background dots. To create DRDS stimuli, a new set of stimulus dots was generated on each movie frame, which eliminated monocular motion cues. The background dots remained static throughout the movie. Dynamic random dot stereograms are 100% spatially correlated but temporally uncorrelated, thus the only motion cue is the change of disparity over time. For RDS stimuli, the background and stimulus dots remained unchanged

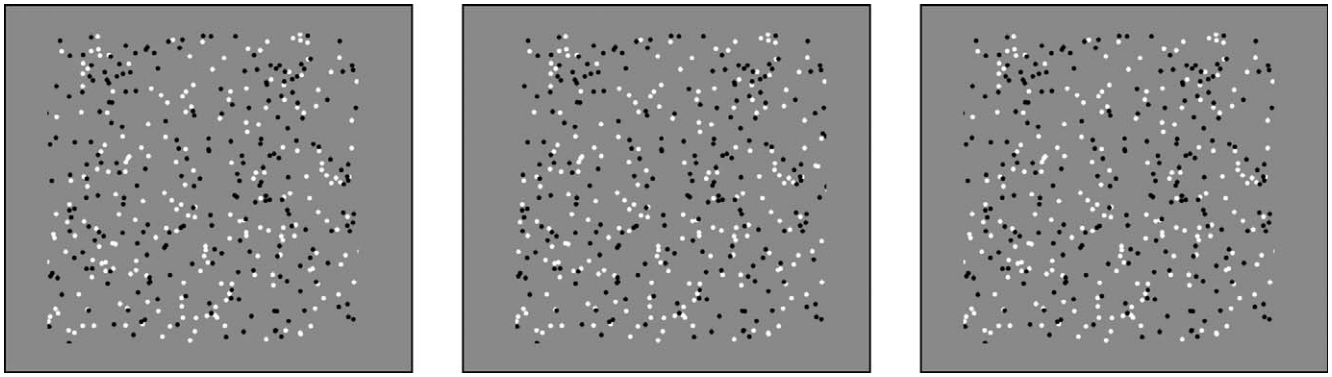

Figure 2. Example stereogram of a single frame from the stimulus movie. Fuse the left and center panels for divergent fusion, and the center and right panels for crossed fusion. A unique random dot pattern was generated for each trial. In DRDS stimuli, new dots within the central rectangle were randomly generated on each frame (120 Hz). For RDS stimuli the dots in the central region were the same throughout the trial. In both RDS and DRDS stimuli the background dots (top and bottom strips) were the same for the duration of each trial. The example image shown here is not gamma-corrected, so differs in luminance and contrast from the experimental stimuli.

throughout the movie, thus two binocular cues to motion in depth were available—changing disparity and interocular velocity difference.

The stimuli were presented through a transparent window (4.9° × 4.9°) centered on the screen, so only the central region of the stimulus was visible. This removed the remaining monocular cues in the DRDS stimuli produced from horizontally shifting the 3D motion dots in each eye's image, as shifted dots that extended further horizontally than the background dots were invisible, and consequently there was no monocular information relating to the extent of the shift. No background dots were placed behind the stimulus dots, so the background dots were only visible above and below the stimulus dots and did not overlap. The initial disparity of the stimulus dots was set to half the disparity extent of the stimulus on that trial (i.e., the midpoint of the motion path of the stimulus dots was zero disparity). To minimize diplopia, the disparity of the background dots during each interval was set at 2.3 arcmin behind the minimum disparity reached by the moving stimulus dots. Thus the disparity of the background dots was different on each trial. The direction of 3D motion in this experiment was always receding motion—no systematic differences between approaching and receding motion have been reported (e.g., Brooks & Stone, 2004).

Two velocities were selected as the standards—0.5 and 1.5 m/s in depth. The duration and total disparity extent (over the range of motion) of each of these standards were as follows: 0.5 m/s (1000 ms and 14 arcmin) and 1.5 m/s (500 ms and 21 arcmin). At this viewing distance, these speeds correspond to horizontal retinal motion of 0.2 and 0.7 deg/s. Velocity in depth was calculated from the change in horizontal disparity over time using Equation 1, where V is velocity in m/s, δ is binocular disparity, t is time, D is viewing distance, and I is interocular distance, approximated as 6.5 cm. The two standard speeds (0.5 and 1.5 m/s) combined with two stimulus types (RDS and DRDS) produced four stimulus conditions, and with thresholds measured in each of the 16 space-time directions (θ), totaled 16 × 4 = 64 experimental conditions.

$$V = \frac{d\delta}{dt} 2D/I \quad (1)$$

Procedure

Observers were seated 2 m from the computer monitor in a dark laboratory with their position fixed using a chin-and-forehead rest, and viewed the computer monitors through a mirror stereoscope. Vergence and eye position was not fixed during motion presentation; instead free viewing of the stimuli was permitted. This was done for the following reasons. Firstly, motion in depth requires a change in relative (not absolute) disparity (Erkelens & Collewijn, 1985a; Regan, Erkelens, & Collewijn, 1986). Secondly, there is evidence that vergence eye movements are not critical (Erkelens, & Collewijn, 1985b; Regan et al., 1986; however, for recent discussion see Harris, 2006, and Lugtigheid, Brenner, & Welchman, 2011) and finally, observers find fixation nearly impossible while viewing motion in depth (e.g., Brooks & Stone, 2004; Harris & Watamaniuk, 1995).

The task was a three-alternative forced choice (3AFC) design. On each trial, three motion-in-depth stimuli were presented sequentially. Two of the stimuli were identical (one of the four standards, 0.5 or 1.5 m/s × RDS or DRDS) and thus had identical spatial and temporal parameters. The third stimulus (the test stimulus) differed in space (disparity), time (duration), or on both dimensions, depending on which angle was being tested (see below). The observer's task was to

discriminate which interval was the odd-one-out. The spatial and temporal parameters of the test stimulus were chosen as a multiple of the standard in a particular direction in space-time. See Figure 1 for a schematic explanation. Just noticeable difference (JND) thresholds for 16 angular directions (θ) away from each standard in space-time were measured: $\theta = 0$ (360), 22.5, 45, 67.5, 90, 112.5, 135, 157.5, 180, 202.5, 225, 247.5, 270, 292.5, 315, and 337.5 degrees. These directions in space-time determined the proportional change in disparity and duration of the test stimulus relative to the standard, and the sign of the change for each parameter (increase or decrease).

On each trial, the three motion-in-depth stimuli were shown sequentially in random order. A 1000 ms interstimulus interval separated each motion movie. After the third stimulus, the screen was cleared to display only a black fixation cross (46.8 × 46.8 arcmin) in the center of the screen. The observer pressed a key to indicate which of the three intervals contained the test stimulus. Feedback was then given by changing the color of the middle bar of the fixation cross to green (correct) or red (incorrect) for 500 ms. The intertrial interval was 1000 ms.

An adaptive staircase (two-up, one-down) method was used to determine the observer's discrimination threshold from the standard in each of the 16 directions in space-time. The staircase terminated after 10 reversals, with the stepsize halved after the fourth reversal. If a staircase failed to reach 10 reversals after 60 trials, it was terminated. The staircase controlled the disparity range and duration of the test stimulus as a multiple of the standard velocity's parameters on each trial. In effect, the staircase determined the threshold for each direction (θ) in terms of vector length away from the standard in space-time. As disparity and duration are in different units, the threshold was determined using proportional increments from the standard in unitless space. In each run, there were two interleaved staircases, θ in opposite directions were included in the same run (i.e., separated by 180°) away from the standard. The advantage was that "slower than" and "faster than" trials were in the same run, so observers could not know whether to look for an increment or decrement on each trial. A minimum of two runs was completed for each condition. Observers completed the runs over several separate sessions.

Data analysis and fitting

Just-noticeable-difference thresholds: Data from each direction (θ) away from the standard were simultaneously fitted with its opposing direction (i.e., $\theta + 180°$) to form a bidirectional psychometric function well described by an inverted Gaussian function (see Figure 3 for an example). The inverted Gaussian is described

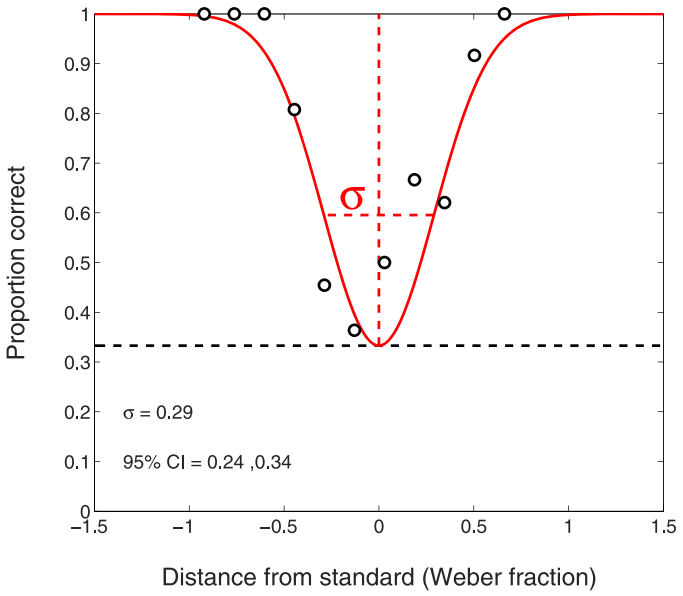

Figure 3. An example inverted Gaussian fit to the data with Equation 1 to obtain a just-noticeable-difference threshold (σ). The example shown is for the standard speed 1.5 m/s RDS for naive observer NM. The Gaussian is simultaneously fit to the data from $\theta = 180°$ and 360° (i.e., $\theta + 180°$) to obtain a bi-directional threshold for this condition. Chance performance on the 3AFC task is indicated by the black dashed line ($\gamma = 0.33$). In this example, the data are binned into proportion correct for clarity. In practice, the thresholds were fitted without binning.

by Equation 2, where α is the horizontal asymptote, A is the amplitude of the peak, b is the center of the peak, and σ is the standard deviation, or width, of the peak. Only the σ parameter was varied in the fitting procedure and the best-fitting σ was used as the threshold (JND) estimate. Because data for the θ and $\theta + 180°$ directions were jointly fit by a single function, the estimated discrimination thresholds for the "slower than the standard" and "faster than the standard" conditions were identical. The σ value is therefore a bi-directional JND threshold for a given directional axis (θ and $\theta + 180°$) around the standard.

The inverted Gaussian was fit to the pooled data from all runs of a condition using the Levenberg-Marquardt algorithm implemented with MATLAB's *nlinfit* routine. The center of the inverted Gaussian was fixed at $b = 0$ as chance performance was expected when the difference between the parameters of the test and standards was minimal. The horizontal asymptote was fixed at $\alpha = 1$ to equal the maximum proportion correct and the height of the peak was set to $A = 1 - \gamma$, where γ is chance performance ($\gamma = 0.33$ for a 3AFC task). Confidence intervals (95%) on the JND thresholds were estimated from the Jacobian matrix using MATLAB's *nlparci* routine.

$$f(x) = -Ae^{-\frac{(x-b)^2}{2\sigma^2}} + \alpha \quad (2)$$

2D threshold contours: Obtaining JND thresholds for the eight directional axes in the way just described produces 16 data points in an approximately elliptical shape around the value of the standard. To obtain the 2D threshold contours ellipses were fit to the sixteen thresholds. This was done separately for each standard velocity and for each observer. The equation for an ellipse fitted to the JND thresholds (r) for each experimental condition (θ, the direction away from the standard in space-time) is derived below in three steps, with the final form (Equation 3c) used for fitting the ellipses. The fitted parameters are a and b, the semimajor and semiminor axes, and the angle of rotation of the ellipse (θ_0), which defines the tilt around the Cartesian axes. A weighted fit to the JNDs was performed using MATLAB's *nlinfit* routine with confidence intervals (95%) on the parameters estimated from the Jacobian matrix as described above for the threshold estimates.

The equation for an ellipse with semimajor and semiminor axes (a, b) aligned with the Cartesian axes (x, y) and with its center at the origin (0, 0) is given by:

$$\frac{x^2}{a^2} + \frac{y^2}{b^2} = 1 \quad (3a)$$

which can be rearranged by substituting $x = r\cos\theta$ and $y = r\sin\theta$ to give:

$$r^2 = \frac{1}{\frac{\cos^2\theta}{a^2} + \frac{\sin^2\theta}{b^2}} \quad (3b)$$

and with the inclusion of an extra term (θ_0) to define the tilt of the ellipse with respect to the Cartesian axes the final form of the equation used for fitting the threshold contours is:

$$r^2 = \frac{1}{\frac{\cos^2(\theta-\theta_0)}{a^2} + \frac{\sin^2(\theta-\theta_0)}{b^2}} \quad (3c)$$

Results and discussion

In this experiment, observers discriminated the "odd-one-out" motion in depth relative to a standard motion in a 3AFC task. The discrimination thresholds (Weber fractions) are plotted in space-time relative to the parameters of the standard motion in each condition (Figure 4). The JNDs for RDS and DRDS stimuli fall in a similar range for observers SW and NM. For observer CL, JNDs have a much broader range for DRDS stimuli compared to RDS, however, observers NM and SW had participated in a pilot experiment for this task using similar DRDS stimuli and were therefore more practiced. For RDS stimuli at 0.5 m/s, JNDs were in the range 0.43–0.57 for NM, 0.27–0.60 for SW and 0.44–0.80 for CL across directions in space-time (θ). Thresholds for discrimination of the faster speed of RDS (1.5 m/s) were comparable, in the range 0.29–0.54 for NM, 0.27–0.67 for SW, and 0.43–0.84 for CL.

The values were similar for the DRDS stimuli. JND thresholds at the slowest speed of 0.5 m/s were between 0.37–0.62 for NM, 0.33–0.52 for SW, and 0.39–3.38 for CL. At the faster speed of 1.5 m/s, DRDS thresholds were 0.40–0.61 for NM, 0.30–0.82 for SW, and 0.31–1.35 for CL. The very high JNDs for CL and DRDS occur at $\theta = 180°$ and 22.5° for both standard speeds, conditions in which duration did not vary between test and standard stimuli ($\theta = 180°$) or provided little information for discrimination ($\theta = 22.5°$). This indicates that CL had a greater reliance on duration than disparity as a discrimination cue for DRDS.

The threshold contours are shown in Figure 4 for each observer and condition. For the RDS stimuli containing both changing disparity and intraocular velocity difference cues, speed tuning is evident for some observers and conditions. Speed tuning is revealed by fitted threshold contours that have a tilt (θ_0) of approximately 45°, along the line of constant velocity in space-time. The fitted values for the tilt of the threshold contours (θ_0) are shown in Figure 5. At the standard speed of 0.5 m/s for RDS, the fitted parameters reveal speed tuning for the two naive observers CL [$\theta_0 = 42.7°$ (95% CI: 35.7, 49.8)] and NM [$\theta_0 = 51.4°$ (95% CI: 41.2, 61.6)], but not for author SW [$\theta_0 = 77.7°$ (95% CI: 70.3, 85.2)]. The contour for SW is elongated along the time axis, indicating better discrimination for displacement than duration. At the faster speed of 1.5 m/s RDS, only the contour for observer CL shows any evidence of speed tuning [$\theta_0 = 58.3°$ (95% CI: 44.2, 72.4)]. For both observers NM [$\theta_0 = 78.7°$ (95% CI: 70.5, 87.0)] and SW [$\theta_0 = 92.1°$ (95% CI: 86.6, 97.5)], the contours for this speed are approximately aligned with the time axis at 90° because discrimination performance was better for displacement (i.e., disparity).

In contrast to RDS stimuli, there is no evidence of speed tuning for DRDS stimuli. The threshold contours for CL reveal a strong preference for duration over displacement for both speeds of DRDS stimuli [0.5 m/s: $\theta_0 = 187.6°$ (95% CI: 186.4, 188.9); 1.5 m/s: $\theta_0 = 187.6°$ (95% CI: 181.6, 193.7)]. The contour for NM is also elongated along the disparity axis at the slower DRDS speed 0.5 m/s [$\theta_0 = 181.7°$ (95% CI: 168.3, 195.2)], evidence for better duration discrimination. However, the contour for NM at the faster speed of 1.5 m/s approximates a circle (note the wide confidence

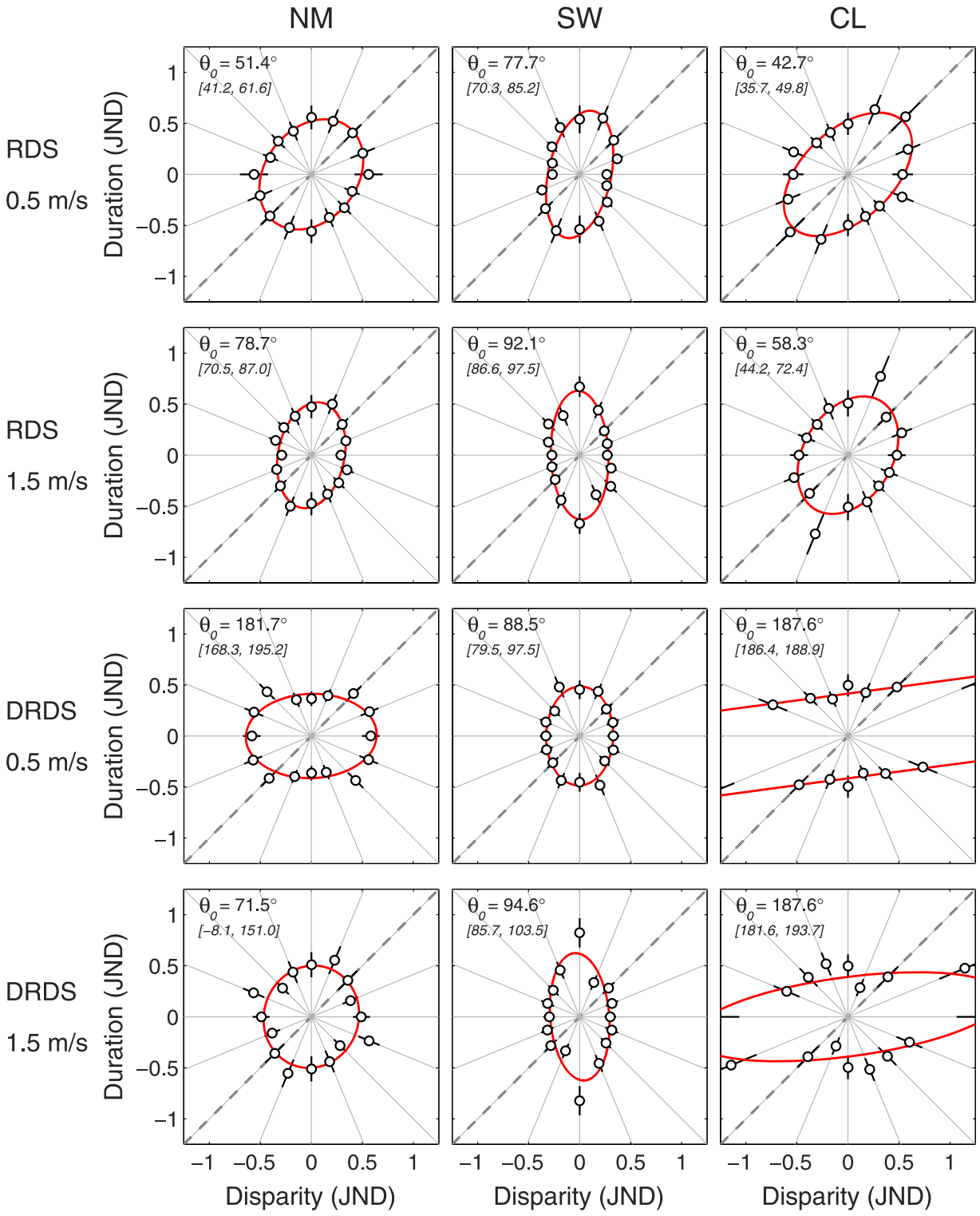

Figure 4. JND threshold contours for the four conditions (rows) and three observers (columns). The data were plotted as the ratio of duration and disparity relative to the parameters of the standard stimulus in each condition (Weber fractions). Circles (black) mark the JNDs in 16 directions away from the standard in stimulus space. Error bars are the 95% confidence intervals on the thresholds. The diagonal dashed line represents the line of constant velocity. Red lines show the (weighted) best-fitting ellipse to the 16 JNDs centered at the origin, using Equation 3c. The value of the tilt parameter (θ_0) from the best-fitting ellipse is shown in the top-left of each graph, with 95% confidence intervals on the tilt estimate in square brackets.

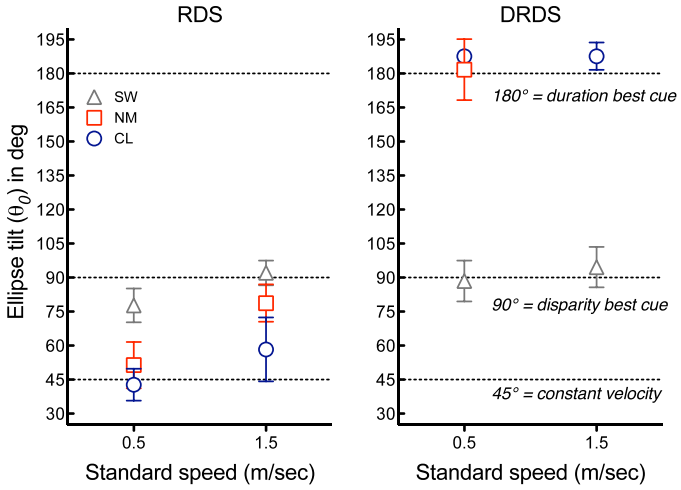

Figure 5. Value of the fitted parameter for the ellipse tilt (θ_0) of the weighted fits to Equation 3c, for each observer and condition in Experiment 1. Error bars are 95% confidence intervals on the parameter estimates. The data point for observer NM at 1.5 m/s DRDS is omitted from the plot because the fitted ellipse approximated a circle (see text for details).

interval indicating that a tilt parameter could not be fitted), evidence that this observer was able to exploit the two cues of disparity and duration equally for discrimination [θ_0 = 71.5° (95% CI: −8.1, 151.0)]. Observer SW shows the inverse pattern to the two naive observers, with threshold contours elongated along the duration axis, indicating disparity was the preferred cue for discrimination at both speeds [0.5 m/s: $\theta_0 = 88.5°$ (95% CI: 79.5, 97.5); 1.5 m/s: $\theta_0 = 94.6°$ (95% CI: 85.7, 103.5)].

The fitted parameters for the semimajor and semiminor axes (a, b) of the threshold contours fitted to Equation 3c are shown in Table 1. The relative size of these parameters indicates the degree of the bias in discrimination between the cues of duration, disparity, and speed. The semimajor axis is the length of the longest axis (along the direction of tilt) and the semiminor axis is the smallest width of the ellipse, which is orthogonal to the major axis. For example, the values of the semimajor and minor axes ($a = 0.51$, $b = 0.46$) are very similar for observer NM for DRDS 1.5 m/s because the threshold contour approximates a circle, evidence of a uniform level of discrimination across cues. However there is a large difference between the two parameters ($a = 1.56$, $b = 0.39$) for observer CL in this condition as discrimination from duration was much better than from disparity.

Experiment 2

In Experiment 1, there was evidence of speed sensitivity to motion in depth for RDS (especially for the slow speed) but not for DRDS. It was also clear from the particularly narrow ellipses that observers sometimes relied strongly on one of the speed components, variously disparity or duration depending on condition and observer. In Experiment 2, we examine speed sensitivity further by degrading the reliability of the separate displacement (disparity) and duration components in the discrimination task with the addition of noise. Following the logic applied in Reisbeck and Gegenfurtner (1999), we add noise to the two standard stimuli while maintaining a constant velocity. As illustrated in Figure 6a, on each trial the space and time components of the two standards are randomly selected along the axis of constant velocity. This means that the standard stimuli are equal in speed, but have different spatial and temporal components. The parameters of the test stimulus are adjusted along one of the five angular directions (θ) away from the mean parameters of the standard to measure the JND. As a result, the test stimulus also has different space and time components than either of the two standards, but additionally differs in speed. Therefore speed is the most useful discrimination cue for selecting the test stimulus on the "odd-one-out" task. The exception is for $\theta = 45°$, as all three stimuli are equal in speed. If speed sensitivity exists for changing disparity over time it should be revealed in this version of the task in which the displacement and duration components are unreliable.

	NM		SW		CL	
	a	*b*	*a*	*b*	*a*	*b*
0.5 m/s RDS	0.59 *[0.55, 0.63]*	0.45 *[0.43, 0.47]*	0.64 *[0.53, 0.74]*	0.31 *[0.28, 0.33]*	0.75 *[0.67, 0.83]*	0.44 *[0.41, 0.47]*
1.5 m/s RDS	0.52 *[0.47, 0.58]*	0.33 *[0.30, 0.35]*	0.63 [0.56, 0.70]	0.28 *[0.26, 0.30]*	0.62 *[0.54, 0.70]*	0.44 *[0.40, 0.47]*
0.5 m/s DRDS	0.64 *[0.56, 0.72]*	0.41 *[0.37, 0.46]*	0.49 *[0.44, 0.53]*	0.33 *[0.31, 0.35]*	—	0.41 *[0.39, 0.43]*
1.5 m/s DRDS	0.51 *[0.41, 0.60]*	0.46 *[0.40, 0.53]*	0.63 *[0.48, 0.77]*	0.29 *[0.25, 0.33]*	1.56 *[0.98, 2.13]*	0.39 *[0.33, 0.45]*

Table 1. The semimajor and semiminor axes (a, b) of the ellipses fitted to the JND thresholds for each observer and standard speed using Equation 3c. The semimajor axis is defined as a if $a > b$, and b if $b > a$. Italicized numbers in brackets are 95% confidence intervals on the parameter estimates. The missing value for observer CL at 0.5 m/s DRDS is because the parameter for the semimajor axis could not be fitted due to extreme threshold values along the disparity axis—see Figure 4.

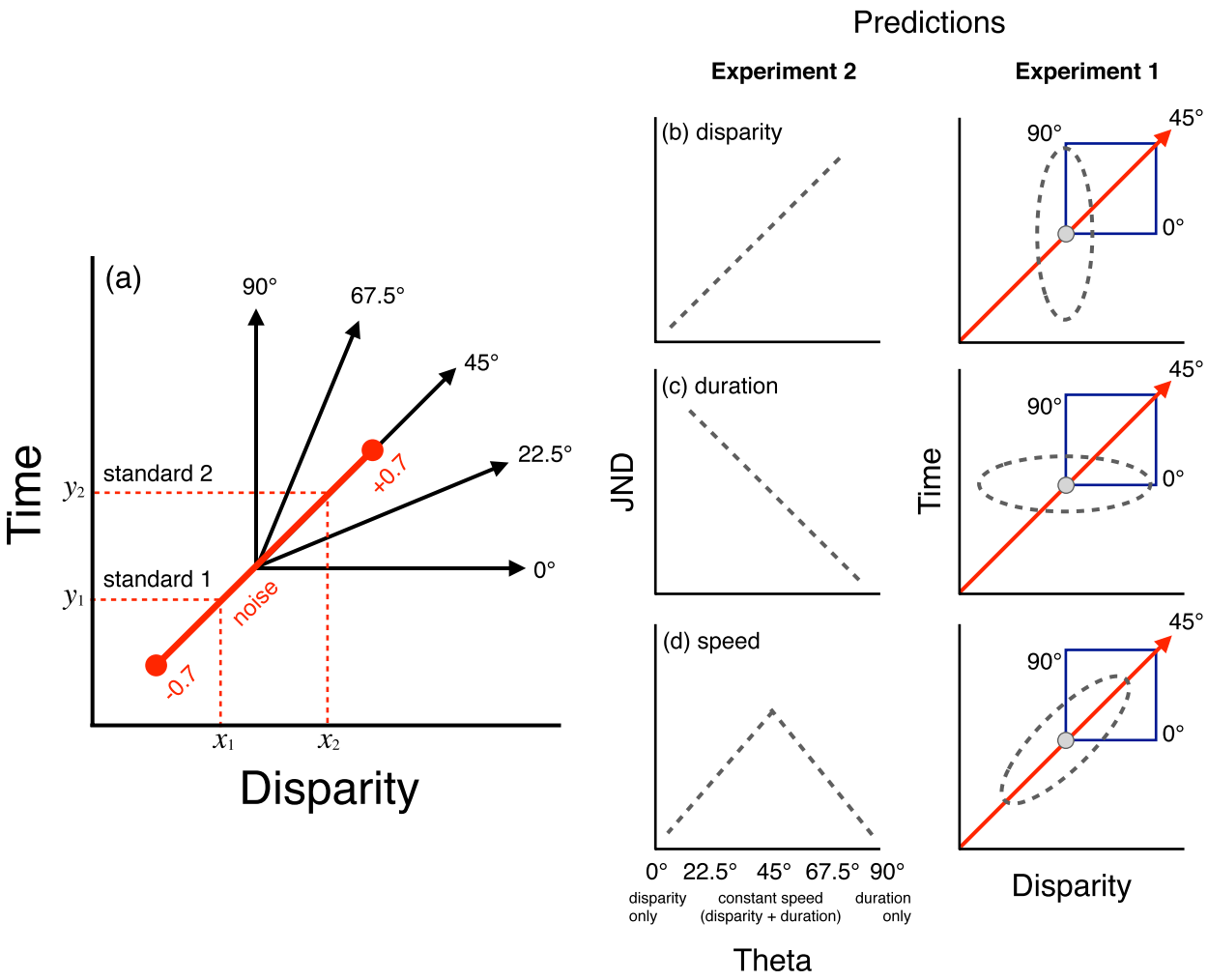

Figure 6. Design and predicted outcomes of Experiment 2. (a) Thresholds are measured in five directions (θ) away from the standard stimuli in space-time, which correspond to different amounts of change in disparity and duration relative to the standard speed (*x*-axis). The diagonal red line in (A) indicates the range of the noise of constant velocity that was added to each of the standards in every condition (θ). On each trial, the parameters of the two standards were randomly selected from a point on this constant velocity line. This corresponds to different spatiotemporal parameters for each standard, but an equal speed. The parameters of standard 1 are given by x1, y1, and the parameters of standard 2 by x2, y2. Predicted data for Experiment 2 are shown by the grey dashed line in each subplot (c, d). To allow for comparison of the design with Experiment 1, next to each subplot is the corresponding predicted threshold contour from Experiment 1, with the quadrant tested in Experiment 2 outlined in blue. If observers preferentially use displacement (disparity) (b) or duration (c) to discriminate the odd-one-out motion, JND thresholds will be lowest for the condition (θ) which changes only this cue, and highest for the other cue. (d) If observers are using speed to discriminate, thresholds will be highest in the $\theta = 45°$ condition when speed is constant (disparity and duration of the test stimulus is changed in equal amounts). A combination of these predictions is possible depending on the extent to which observers use each cue for discrimination.

The design of the discrimination task was altered in Experiment 2 because of the limitations of simulating motion in depth in the laboratory. In order to add a random amount of noise of constant velocity to each standard motion, a larger stimulus space is required than was available. The reason is that adding random jitter to the disparity and duration components expands the range of parameter values that might be required on a given trial, causing two problems. First, if the values of disparity or duration are too low, the stimulus appears static and the task is no longer motion discrimination, and if the parameters take very large values, diplopia becomes an additional discrimination cue. Second, the usable range of parameter values must leave sufficient space to adjust the test stimulus parameters to measure a threshold. In order to maximize the amount of noise added to the standard within these restrictions we tested discrimination in one direction only (i.e., one quadrant in space-time, rather than the full ellipse. See Methods).

The design and predictions of Experiment 2 are shown in Figure 6. The two standard stimuli on each

trial now occupy different positions in space-time along the line of constant velocity (red line in Figure 6a), and JND thresholds are measured in five directions away from the standards (relative to the original parameters of the standards as used in Experiment 1—i.e., the mean of the uniform noise distribution that the two standards are drawn from). It is possible to distinguish between which cues observers use to make the discrimination based on the pattern of results across conditions (Figure 6b through d). If observers use disparity for discrimination, thresholds should be lowest for conditions in which the change in disparity is greatest ($\theta = 0$, 22.5). This pattern will be reversed if observers favor duration as a discrimination cue (Figure 6c), and thresholds will be lowest for the directions in space-time in which duration changes more rapidly ($\theta = 67.5$, 90). If observers discriminate based on speed (which is the most reliable cue in Experiment 2), thresholds will peak at $\theta = 45$, when the speed of the test stimulus equals that of the two standards, and the less reliable component cues of displacement (disparity) and duration must be used instead (Figure 6d).

Method

Observers

The same three observers from Experiment 1 participated.

Apparatus and stimuli

The experimental setup and stimuli were identical to Experiment 1, except for the following modifications. In this experiment the standard stimuli had the same speed as in Experiment 1, but different spatial and temporal parameters on each trial, and to each other, because of the addition of noise. The same mean speeds for the standards were used as in Experiment 1: 0.5 m/s (1000 ms and 14 arcmin) and 1.5 m/s (500 ms and 21 arcmin) in depth. However, the duration and total disparity extent were selected from uniform distributions along the line of constant velocity in space-time, centered on these mean values and spanning −0.7 to +0.7 (−70% and +70%) Weber fraction in constant velocity jitter (Figure 6a). For the standard of 0.5 m/s the parameters were randomly selected between 508–1492 ms in duration and 7–21 arcmin in disparity extent on each trial. For the standard of 1.5 m/s the parameters were between 250–750 ms and 11–31 arcmin.

The JND thresholds were measured only for the five "increment" conditions from Experiment 1—i.e., an increase in duration, disparity or both parameters, relative to the mean values of the standard. In space-time this corresponds to the theta values of $\theta = 0°$, 22.5°, 45°, 67.5°, and 90° (Figure 6). The starting disparity of each of the two standard stimuli in each trial was selected from a uniform distribution between ±10 arcmin near or far disparity relative to the screen (zero disparity). This was to prevent the test stimulus having the greatest starting disparity more often (as increments only were being tested). In addition, the disparity of the background dot surface was also randomly selected from a uniform distribution between 0.58 arcmin and 10 arcmin.

Data analysis and fitting

Just-noticeable-difference thresholds: Psychometric functions were fit to the data separately for each condition and observer with a cumulative Gaussian function, using the Levenberg-Marquardt algorithm implemented with MATLAB's *nlinfit* routine. The standard deviation of the fitted function was taken as the threshold estimate and confidence intervals (95%) on the threshold estimates were derived from the Jacobian matrix of the fitted function with MATLAB's *nlparci* routine.

Results and discussion

JND thresholds for discrimination of motion in depth were measured with noise of constant velocity added to the standard motion, for one quadrant (five directions) in space-time (Figure 6a). Thresholds for the tasks in Experiment 1 and Experiment 2 are not directly comparable because two directions of motion discrimination ("slower than" and "faster than") were simultaneously measured in Experiment 1, and only one direction ("faster than") was measured in Experiment 2. For RDS patterns at 0.5 m/s, JND thresholds were in the range of 0.64–0.99 for observer NM, 0.43–0.90 for SW, and 0.31–0.80 for CL. At 1.5 m/s, thresholds were 0.43–1.31 for NM, 0.45–1.18 for SW, and 0.57–1.05 for CL. The ranges for DRDS stimuli were comparable. For 0.5 m/s, 0.62–1.99 for NM, 0.54–1.00 for SW, 0.61–1.01 for CL. For 1.5 m/s, thresholds were between 0.79–1.47 for NM, 0.39–1.52 for SW, and 0.64–1.24 for CL.

Elliptical threshold contours were not fitted to the data in Experiment 2 because only one quadrant in space-time was tested. Figure 6 illustrates the predictions for the pattern of data that would indicate speed sensitivity, or reliance on one of the components—displacement (disparity) or duration. The thresholds for each observer and condition are shown in Figure 7. For the 0.5 m/s RDS stimuli, the pattern of results is indicative of speed tuning—thresholds for the two naive observers (NM, CL) peak at $\theta = 45°$ when the speed of both standards and the test pattern is equal.

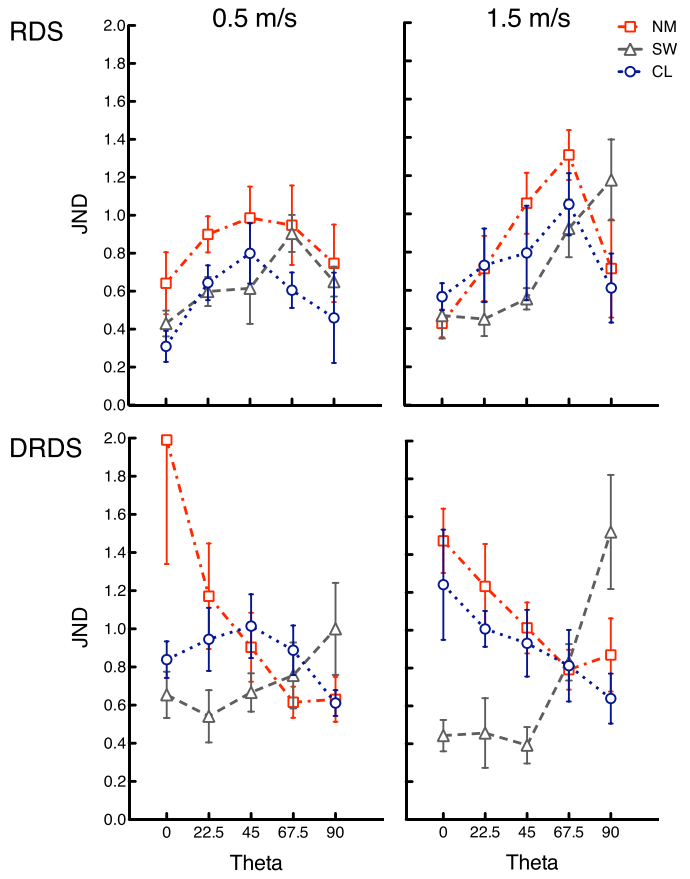

Figure 7. JND thresholds for the four conditions in Experiment 2. Thresholds were measured in five directions (θ) away from the standard stimuli in space-time. Individual data for all three observers are shown. Error bars are the 95% confidence intervals on the thresholds.

The peak for observer SW is slightly offset at $\theta = 67.5°$ but the pattern is similar. For the standard speed of 1.5 m/s, the pattern is less clear. The thresholds peak at $\theta = 67.5°$ for observers NM and CL. For observer SW, thresholds increase in line with a reliance on disparity for discrimination (Figure 5a). Overall, the pattern of results for RDS stimuli is consistent with that in Experiment 1—there is evidence for speed tuning for the slower RDS standard speed (0.5 m/s) and limited suggestion of speed tuning at the faster speed (1.5 m/s).

Overall the pattern of results for DRDS stimuli is not indicative of speed tuning. The one exception is for observer CL at 0.5 m/s—thresholds peak at $\theta = 45°$. For NM the pattern for 0.5 m/s is consistent with a reliance on duration, as thresholds systematically increase for conditions in which the change in disparity is greater than that in duration, with a peak at $\theta = 0°$, when disparity is the only cue and duration is held constant. For SW at 0.5 m/s thresholds increase moderately as duration becomes the more useful cue, indicative of a reliance on disparity. For the faster speed of 1.5 m/s DRDS there is clearly no evidence of speed tuning. Observers NM and CL are relying on duration as a discrimination cue, with better discrimination performance in conditions with a greater rate of change in duration, peaking at $\theta = 90°$ when only duration changes and displacement (disparity) is held constant. The pattern for SW is the inverse, with the lowest thresholds when disparity is the most informative cue ($\theta = 0°$).

General discussion

We measured 2D threshold contours in space-time for the discrimination of motion in depth for RDS stimuli containing two binocular cues to motion—interocular velocity difference (IOVD) and changing disparity over time, and for DRDS stimuli containing only the changing disparity cue. The "odd-one-out" task required observers to discriminate the motion of the test stimulus from two identical standard stimuli in a 3AFC procedure. Discrimination thresholds were measured in different directions in space-time away from the parameters of the standard motion. The advantage of this paradigm is that the shape of the threshold contours reveals the extent to which observers used the individual cues of disparity, duration, and speed to discriminate motion in depth.

Evidence for speed sensitivity was found for RDS stimuli at the standard speed of 0.5 m/s, as threshold contours for two out of three observers were aligned along the constant speed axis (45° in space-time) in Experiment 1. Speed sensitivity was not observed for faster RDS stimuli at 1.5 m/s, or for DRDS stimuli of either speed. These results were confirmed in Experiment 2, in which random noise of constant velocity was added to the standard motions, thereby degrading the reliability of the separate disparity and duration components as discrimination cues. As in Experiment 1, there was evidence in the pattern of threshold elevation that observers were using speed to discriminate RDS stimuli at 0.5 m/s and some evidence for 1.5 m/s, but not for DRDS stimuli at either speed. There was an exception for one observer (CL) who showed some speed tuning for DRDS stimuli at the slower speed, but this was not the case for the other observers. Together the results suggest that IOVD is the critical cue for speed discrimination of motion in depth.

In both Experiments 1 and 2, there were considerable individual differences in the relative ability of the three observers to exploit the component cues of disparity and duration for stereomotion discrimination. For example, for DRDS stimuli in Experiment 1, observer SW was better at discriminating stereomotion based on changes in disparity than the other two observers, indicated by this observer's lower thresholds for

conditions in which disparity was the most informative cue (around $\theta = 180°$). This may be an effect of training because this observer was the most practiced at the task. Similarly, observer NM, who had practiced in a similar pilot experiment with DRDS stimuli, had lower discrimination thresholds for conditions in which disparity was the most informative cue than inexperienced observer CL, who had never previously discriminated DRDS stimuli. Thus the experience of observers appears to relate to their ability to use disparity as a discrimination cue for motion in depth. Interestingly, this pattern was the reverse for the speed tuning observed for RDS stimuli. Speed tuning was most clear in the data for the least experienced observer CL, and speed tuning was not evident for the most experienced observer SW. It may be the case that experienced observers who have learned to use the component cue of disparity for discrimination are able to compensate by using this cue in the speed condition ($\theta = 45°$), thus no threshold elevation is observed, which obscures the presence of any speed tuning. This is a limitation of the design of the threshold contour paradigm: if observers are too good at using the component cues for motion discrimination, speed tuning may not be revealed even if it is present.

Speed discrimination of motion in depth

The size of the JND thresholds in Experiment 1 are comparable to that in other studies of speed discrimination of 3D motion, however, performance cannot be directly compared because the threshold contour paradigm and odd-one-out task is substantially different from previous studies of speed discrimination. Previous investigations of stereomotion speed perception have used two-interval forced choice tasks, in which observers select the interval containing the faster 3D motion (Brooks & Stone, 2004; Harris & Watamaniuk, 1995; Portfors-Yeomans & Regan, 1996; Portfors & Regan, 1997). The following thresholds are for motion either directly towards or away from the observer. Harris and Watamaniuk (1995) reported Weber fractions for speed discrimination of RDS stimuli between 0.1–0.2, and similarly, thresholds were approximately 0.1–0.25 in Brooks and Stone (2004), 0.093–0.15 in Portfors-Yeomans and Regan (1996), and 0.07–0.20 in Portfors and Regan (1997). In Experiment 1 in this paper, Weber fractions for RDS stimuli had greater variability, between 0.27–0.80 for the standard speed of 0.5 m/s and 0.29–0.84 for 1.5 m/s, across observers and conditions.

The wider range in thresholds for discrimination of RDS stereomotion in Experiment 1 compared to previous studies is explained by significant differences between the tasks. Rather than straightforward speed discrimination, which is compromised by the fact that observers may use cues other than speed, our paradigm was designed to reveal speed sensitivity indirectly by comparing observers' ability to discriminate 3D motion for different weightings of speed, disparity and duration. Thus our experiment was a *motion* discrimination task rather than the *speed* discrimination task used in the previous experiments. In fact speed was not even an available cue in one condition ($\theta = 45°$) as the speed of the test and standard stimuli were equal. As the rate of change of disparity, duration and speed in the test stimulus relative to the standard varied between conditions, it is unsurprising that thresholds for discrimination varied as a function of observers' ability to use the individual cues. Despite the significant differences in experimental design, the lowest Weber fractions of 0.27–0.29 measured here for motion discrimination of RDS stimuli are similar to the upper limit of 0.2–0.25 for speed discrimination in previous experiments (Harris and Watamaniuk, 1995; Brooks and Stone, 2004; Portfors and Regan, 1997).

An inconsistency among 3D motion experiments is that while some find a clear advantage in speed discrimination thresholds for RDS compared to DRDS stimuli (Brooks & Stone, 2004; Harris & Watamaniuk, 1995), this is not evident in others (Portfors-Yeomans & Regan, 1996, Portfors & Regan, 1997), including the present paper. In Harris and Watamaniuk (1995) Weber fractions for speed discrimination in DRDS stimuli were at least 2.5 times higher than those for RDS. Similarly, Brooks and Stone (2004) reported DRDS thresholds 1.4–2.4 times higher than for RDS. Weber fractions for stereomotion speed discrimination in DRDS stimuli were approximately 0.4–0.5 in Harris and Watamaniuk (1995) and 0.25–0.6 in Brooks and Stone (2004). Thresholds were considerably lower in the experiments that did not find an advantage for RDS stimuli—0.091–0.22 in Portfors-Yeomans and Regan (1996), and 0.07–0.17 in Portfors and Regan (1997). In contrast, in the current study thresholds ranged between 0.33–3.38 and 0.30–1.35 for 0.5 m/s and 1.5 m/s DRDS stimuli respectively. The wide range is because observer CL had much higher thresholds for DRDS stimuli along the disparity axis—with the two outlier conditions removed for CL ($\theta = 22.5°$ and 180°), DRDS thresholds are less variable, 0.33–0.80 for 0.5 m/s and 0.30–0.80 for 1.5 m/s. This range is nearly identical to the RDS thresholds in Experiment 1, so there is no clear distinction in thresholds for the two stimuli types.

The contradiction across studies can be reconciled by an examination of the methods. As pointed out in Brooks and Stone (2004), the reason for the comparable RDS and DRDS discrimination thresholds in Portfors-Yeomans and Regan (1996) and Portfors and Regan (1997) is most likely because of an

inadequate IOVD cue in their RDS stimuli. The individual dots in their stimuli did not carry a cue to IOVD because they were modified versions of the DRDS stimuli on a blank or stationary background. As for the current study, a consequence of the variability in the relative contribution of the motion cues between conditions is that the experimental design is not appropriate for this comparison. Differences in the absolute magnitude of the thresholds for the two stimuli types are likely to be masked by compensation from the component cues when speed discrimination is difficult. However, as will be discussed in the next section, we do find a difference in speed sensitivity revealed by the shape of the threshold contours. Thus in general it appears there is a benefit for speed discrimination in RDS stimuli from the addition of the IOVD cue, when the task and stimuli are appropriate for this comparison.

The standard speeds in Experiments 1 and 2 span the range used in previous stereomotion experiments. In general slow speeds have been used, particularly in earlier experiments, because of the restricted display range for motion in depth simulation in the laboratory. The units used to express the speed of motion in depth are not consistent—some authors use horizontal retinal image motion, and others *z-axis* speed in depth (see Equation 1). Our standard speeds of 0.5 m/s and 1.5 m/s in depth correspond to horizontal retinal image speeds of 0.2 and 0.7 deg/s (Equation 1). Harris and Watamaniuk (1995) used a standard of 0.32 m/s—a slightly slower *z*-axis speed than our lower limit (0.5 m/s). Portfors and Regan (1997) used a retinal image speed of 0.25°/s, equivalent to our slowest standard (0.2°/s). Brooks and Stone (2004, 2006) used a standard retinal image speed of 0.62°/s, comparable to our fastest standard at 0.7°/s. The clearer pattern of speed sensitivity in our data for the slower speed (0.5 m/s) in Experiments 1 and 2 suggests that speed sensitivity may in fact be more evident for slower 3D motion speeds, and observers may be more likely to rely on the component cues of displacement and duration at faster speeds.

Comparison of binocular cues: Speed sensitivity requires IOVD

The results of Experiments 1 and 2 imply that IOVD is the critical cue for speed sensitivity to motion in depth, with little or no contribution from changing disparity over time. This does not necessarily rule out the possibility that speed can be discriminated in stimuli lacking IOVD cues (such as DRDS). However, it implies that speed discrimination for stimuli without IOVD would have to be supported by an indirect computation of speed via *static* disparity mechanisms, rather than mechanisms tuned to changes in disparity over time.

The importance of IOVD in speed discrimination has been emphasized in previous studies. In addition to lower speed discrimination thresholds for RDS, there is evidence that observers do not use speed for discrimination in DRDS. Harris and Watamaniuk (1995) varied stimulus duration as a control in their speed task, and found that observers tended to select the longer duration DRDS stimulus as "faster." This indicates that observers were using a position cue based on static disparity for discrimination of DRDS rather than speed. In contrast, this bias was not evident for RDS, suggesting that observers were using speed. These results are in agreement with our experiments. Threshold contours were generally elongated along the speed axis for slow RDS stimuli, but along the disparity or duration axes for DRDS, evidence that observers were using speed for discrimination of RDS and the separate cues of displacement or duration for DRDS. This was replicated in Experiment 2, as observers did not appear to use speed to discriminate DRDS even when the reliability of duration and displacement cues was compromised by the addition of noise of constant speed to the standard stimuli.

Brooks and Stone (2004) also varied stimulus duration as a control, yet in their experiment there was no systematic response bias based on duration or displacement in RDS or DRDS stimuli. However, they still found superior speed discrimination for RDS. Additionally, stereoacuity for the two stimuli were equivalent, evidence that it is IOVD that affords the benefit in speed discrimination. In a careful analysis based on stimuli of different trajectories, Brooks and Stone (2004) were also able to rule out several alternative strategies for discrimination of RDS, highlighting the importance of the IOVD cue for speed discrimination.

However, because RDS actually contain both binocular cues, it is possible that changing disparity contributes to speed sensitivity in conjunction with IOVD, but is not a sufficient cue in isolation. It is possible to design stimuli which attempt to isolate IOVD by removing the disparity signal, either by using uncorrelated dot patterns in each eye (e.g., Brooks, 2002; Shioiri et al., 2000), or anticorrelated stimuli in which the luminance of the dots is reversed in each monocular half-image (e.g., Czuba, Rokers, Huk, & Cormack, 2010; Harris & Rushton, 2003; Rokers, Cormack, & Huk, 2008). However, detection performance for motion direction in uncorrelated patterns does not reach 100% even at high contrast (Shioiri et al., 2000). Another problem with uncorrelated dot patterns is that there is the possibility of spurious disparity matching between individual dots in the uncorrelated monocular images. Although there is also

the possibility of spurious coherent motion signals in DRDS, the large number of frames (e.g., 120 Hz display rate in our experiments) makes it much less likely than spatial matching in uncorrelated RDS, which have only two images, one for each eye (Harris et al., 2008). Nefs and Harris (2010) have shown that observers generally do not perceive displacement in two-frame motion displays containing only IOVD, although they can for displays with only changing disparity. Similarly, motion in depth in anticorrelated displays is typically perceived without any corresponding change in position (Rokers et al., 2008). In addition, the elimination of the percept of depth in anticorrelated dot patterns does not guarantee that there is no neural response from disparity detectors (Cumming & Parker, 1997; Harris & Rushton, 2003). Thus it is more difficult to isolate the IOVD cue than changing disparity, which is why many experiments rely on the comparison between RDS and DRDS.

The importance of IOVD in speed sensitivity is also supported by 3D motion adaptation experiments. A 3D motion aftereffect has been demonstrated that is not reducible to adaptation of the component 2D motions (Czuba et al., 2011). A strong 3D motion aftereffect is reported from IOVD stimuli, with weak or no aftereffects reported from changing disparity (Czuba et al., 2011, 2012; Sakano et al., 2012). Similarly, Brooks (2002) found that IOVD was critical for the related velocity aftereffect, which causes a reduction in perceived speed following adaptation. Brooks (2002) compared the effects of adaptation using stimuli containing one or both cues and found that the aftereffect from RDS and uncorrelated RDS (containing only IOVD) was equally effective, supporting the importance of the IOVD cue for speed sensitivity.

The relative importance of IOVD and changing disparity as cues for 3D motion perception is likely to vary under different viewing conditions. For example, as stereoacuity declines in the periphery (McKee, 1983; Rawlings & Shipley, 1969; Wardle, Bex, Cass, & Alais, 2012) it might be expected that IOVD may be a more useful cue for motion away from the fovea. This has indeed been found for 3D motion direction discrimination, as sensitivity to changing disparity is highest in the fovea at slow speeds, and IOVD sensitivity increases at higher speeds and is maintained at a greater range of eccentricities (Czuba, Rokers, Huk, & Cormack, 2010). A difference in speed sensitivity between IOVD and changing disparity also varies with spatial scale. Brooks and Stone (2006) found that speed discrimination rapidly declines for DRDS stimuli with decreasing stimulus size, yet performance remains stable for RDS over a larger range of spatial scales. Interestingly, individual differences in sensitivity to IOVD and changing disparity have been measured (Nefs, O'Hare, & Harris, 2010); suggesting that sensitivity to the two cues also varies across observers.

An important question is whether the speed sensitivity observed in RDS stimuli is evidence for specific binocular mechanisms tuned to the speed of motion in depth. A limitation of the threshold contour paradigm used here is that it cannot distinguish between low-level sensory mechanisms and higher-level decision processes. The existence of speed-tuning for RDS stimuli at slow speeds does not necessarily demonstrate the existence of low-level binocular mechanisms tuned to speed, because it is possible that a higher-level mechanism extracts speed based on separate responses to the components of disparity displacement and duration. The threshold contour paradigm is unable to distinguish between these alternatives. However, what is clear is that under some conditions, observers can judge the speed of 3D motion from binocular cues alone, and that this ability relies upon the IOVD cue.

Summary and conclusions

Measurement of 2D threshold contours for the discrimination of motion in depth revealed differential speed sensitivity for two binocular cues to 3D motion – IOVD and changing disparity. Observers showed evidence for speed sensitivity in RDS, which contained both cues, particularly at slower speeds (0.5 m/s). In contrast, observers relied on the component cues of displacement and duration for discrimination of DRDS at both slower (0.5 m/s) and faster speeds (1.5 m/s). This difference in sensitivity between RDS and DRDS was robust, as reducing the reliability of the component cues in a second experiment still did not reveal speed sensitivity for DRDS. In addition, there were substantial individual differences in the ability of observers to discriminate motion in depth from the component cues of duration and disparity, and this ability appeared to change with practice. We conclude that speed sensitivity to 3D motion is possible from binocular cues alone, however, it requires the presence of IOVD and is restricted to relatively slow speeds.

Acknowledgments

Commercial relationships: none.
Corresponding author: Susan G. Wardle.
Email: susan.wardle@sydney.edu.au.
Address: School of Psychology, The University of Sydney, Sydney, NSW, Australia.

References

Beverley, K. I., & Regan, D. (1973). Evidence for the existence of neural mechanisms selectively sensitive to the direction of movement in space. *The Journal of Physiology, 235,* 17–29.

Brainard, D. H. (1997). The psychophysics toolbox. *Spatial Vision, 10,* 433–436.

Brooks, K. R. (2002). Interocular velocity difference contributes to stereomotion speed perception. *Journal of Vision, 2*(3):2, 218–231, http://www.journalofvision.org/content/2/3/2, doi:10.1167/2.3.2. [PubMed] [Article]

Brooks, K. R., & Stone, L. S. (2004). Stereomotion speed perception: Contributions from both changing disparity and interocular velocity difference over a range of relative disparities. *Journal of Vision, 4*(12):6, 1061–1079, http://www.journalofvision.org/content/4/12/6, doi:10.1167/4.12.6. [PubMed] [Article]

Brooks, K. R., & Stone, L. S. (2006). Spatial scale of stereomotion speed processing. *Journal of Vision, 6*(11):9, 1257–1266, http://www.journalofvision.org/content/6/11/9, doi:10.1167/6.11.9. [PubMed] [Article]

Brooks, K. R., & Stone, L. S. (2010). Accuracy of stereomotion speed perception with persisting and dynamic textures. *Perceptual and Motor Skills, 111,* 921–935.

Cumming, B. G., & Parker, A. J. (1997). Responses of primary visual cortical neurons to binocular disparity without depth perception. *Nature, 389,* 280–283.

Cumming, B. G., & Parker, A. J. (1994). Binocular mechanisms for detecting motion-in-depth. *Vision Research, 34,* 483–495.

Czuba, T. B., Rokers, B., Huk, A. C., & Cormack, L. K. (2012). To CD or not to CD: Is there a 3D motion aftereffect based on changing disparities? *Journal of Vision, 12*(4):7, 1–3, http://www.journalofvision.org/content/12/4/7, doi:10.1167/12.4.7. [PubMed] [Article]

Czuba, T. B., Rokers, B., Guillet, K., Huk, A. C., & Cormack, L. K. (2011). Three-dimensional motion aftereffects reveal distinct direction-selective mechanisms for binocular processing of motion through depth. *Journal of Vision, 11*(10):18, 1–18, http://www.journalofvision.org/content/11/10/18, doi:10.1167/11.10.18. [PubMed] [Article]

Czuba, T. B., Rokers, B., Huk, A. C., & Cormack, L. K. (2010). Speed and eccentricity tuning reveal a central role for the velocity-based cue to 3D visual motion. *Journal of Neurophysiology, 104,* 2886–2899.

Erkelens, C. J., & Collewijn, H. (1985a). Motion perception during dichoptic viewing of moving random-dot stereograms. *Vision Research, 25,* 583–588.

Erkelens, C. J., & Collewijn, H. (1985b). Eye movements and stereopsis during dichoptic viewing of moving random-dot stereograms. *Vision Research, 25,* 1689–1700.

Fernandez, J. M., & Farell, B. (2005). Seeing motion in depth using inter-ocular velocity differences. *Vision Research, 45,* 2786–2798.

Gray, R., & Regan, D. (1999). Motion in depth: Adequate and inadequate simulation. *Perception & Psychophysics, 61,* 236–245.

Harris, J. M. (2006). The interaction of eye movements and retinal signals during the perception of 3-D motion direction. *Journal of Vision, 6*(8):2, 777–790, http://www.journalofvision.org/content/6/8/2, doi:10.1167/6.8.2. [PubMed] [Article]

Harris, J. M., & Rushton, S. K. (2003). Poor visibility of motion in depth is due to early motion averaging. *Vision Research, 43,* 385–392.

Harris, J. M., & Watamaniuk, S. N. (1995). Speed discrimination of motion-in-depth using binocular cues. *Vision Research, 35,* 885–896.

Harris, J. M., & Watamaniuk, S. N. (1996). Poor speed discrimination suggests that there is no specialized speed mechanism for cyclopean motion. *Vision Research, 36,* 2149–2157.

Harris, J. M., Nefs, H. T., & Grafton, C. E. (2008). Binocular vision and motion-in-depth. *Spatial Vision, 21,* 531–547.

Julesz, B. (1971). *Foundations of cyclopean perception.* Chicago: University of Chicago Press.

Lugtigheid, A. J., Brenner, E., & Welchman, A. E. (2011). Speed judgments of three-dimensional motion incorporate extraretinal information. *Journal of Vision, 11*(13):1, 1–11, http://www.journalofvision.org/content/11/13/1, doi:10.1167/11.13.1. [PubMed] [Article]

McKee, S. P. (1983). The spatial requirements for fine stereoacuity. *Vision Research, 23,* 191–198.

Nefs, H. T., & Harris, J. M. (2010). What visual information is used for stereoscopic depth displacement discrimination? *Perception, 39,* 727–744.

Nefs, H. T., O'Hare, L., & Harris, J. M. (2010). Two independent mechanisms for motion-in-depth perception: Evidence from individual differences. *Frontiers in Psychology, 1*:155, 1–8.

Pelli, D. G. (1997). The VideoToolbox software for visual psychophysics: Transforming numbers into movies. *Spatial Vision, 10,* 437–442.

Portfors, C. V., & Regan, D. (1997). Just-noticeable difference in the speed of cyclopean motion in depth and the speed of cyclopean motion within a frontoparallel plane. *Journal of Experimental Psychology: Human Perception and Performance, 23,* 1074–1086.

Portfors-Yeomans, C. V., & Regan, D. (1996). Cyclopean discrimination thresholds for the direction and speed of motion in depth. *Vision Research, 36,* 3265–3279.

Rashbass, C., & Westheimer, G. (1961). Disjunctive eye movements. *The Journal of Physiology, 159,* 339–360.

Rawlings, S. C., & Shipley, T. (1969). Stereoscopic acuity and horizontal angular distance from fixation. *Journal of the Optical Society of America, 59,* 991–993.

Regan, D. (1993). Binocular correlates of the direction of motion in depth. *Vision Research, 33,* 2359–2360.

Regan, D., Erkelens, C. J., & Collewijn, H. (1986). Necessary conditions for the perception of motion in depth. *Investigative Ophthalmology & Visual Science, 27,* 584–597. [PubMed] [Article]

Regan, D., & Gray, R. (2009). Binocular processing of motion: Some unresolved questions. *Spatial Vision, 22,* 1–43.

Reisbeck, T. E., & Gegenfurtner, K. R. (1999). Velocity tuned mechanisms in human motion processing. *Vision Research, 39,* 3267–3285.

Rokers, B., Cormack, L. K., & Huk, A. C. (2008). Strong percepts of motion through depth without strong percepts of position in depth. *Journal of Vision, 8*(4):6, 1–10, http://www.journalofvision.org/content/8/4/6, doi:10.1167/8.4.6. [PubMed] [Article]

Rokers, B., Cormack, L. K., & Huk, A. C. (2009). Disparity- and velocity-based signals for three-dimensional motion perception in human MT+. *Nature Neuroscience, 12,* 1050–1055.

Sakano, Y., Allison, R. S., & Howard, I. P. (2012). Motion aftereffect in depth based on binocular information. *Journal of Vision, 12*(1):11, 1–15, http://www.journalofvision.org/content/12/1/11, doi:10.1167/12.1.11. [PubMed] [Article]

Shioiri, S., Saisho, H., & Yaguchi, H. (2000). Motion in depth based on inter-ocular velocity differences. *Vision Research, 40,* 2565–2572.

Sumnall, J. H., & Harris, J. M. (2000). Binocular three-dimensional motion detection: Contributions of lateral motion and stereomotion. *Journal of the Optical Society of America A, 17,* 687–696.

Wardle, S. G., Bex, P. J., Cass, J., & Alais, D. (2012). Stereoacuity in the periphery is limited by internal noise. *Journal of Vision, 12*(6):12, 1–12, http://www.journalofvision.org/content/12/6/12, doi:10.1167/12.6.12. [PubMed] [Article]